Progress In Electromagnetics Research B, Vol. 42, 263–289, 2012

A SYNTHESIS METHOD FOR TIME-DOMAIN PASSIVE FILTERS COMPENSATING FOR WAVEFORM DISTORTION

U. Sangawa*

Advanced Technology Research Laboratories, Panasonic Corporation, 3-4 Hikaridai, Seika-cho, Soraku-gun, Kyoto 619-0237, Japan

Abstract—A novel synthesis method for a class of time-domain passive filters that compensates for waveform distortion caused by frequency dependencies of the transmission properties of signal propagation paths, is formulated. The method is based on the linear response theory and mathematical properties of scattering matrices for passive circuits. This paper focuses on the formulation and theoretical consistency of the method. The causal transfer functions for the filters can be extracted by "regularizing" the inverse of a transfer function of the path. To fulfill the necessary restrictions imposed on the causal functions, regularization is realized by multiplying the function of linear phase filters comprising a sufficient number of resonators by the inverse. The filter circuits are easily derived from the regularized transfer functions through numerical optimization techniques and the coupling matrix synthesis method to determine transmission poles and extract each lumped element value, respectively. The method is then applied to practically designing a filter that compensates for the frequency dependencies of a two-port radio propagation path having a pair of wideband antennas. In addition, applications of the filter and the scope of further developments of this technology are discussed.

1. INTRODUCTION

The demand for high data rates has increased rapidly for both wired and wireless communication systems, which is a natural consequence of the increasing volume of data to be transmitted. This trend has led to increased bandwidths being assigned to authorized bands for these systems, which is an inevitable consequence of Shannon's theorem.

Received 10 May 2012, Accepted 17 July 2012, Scheduled 18 July 2012

* Corresponding author: Ushio Sangawa (sangawa.ushio@jp.panasonic.com).

In addition, to maximize the efficiency of frequency utilization, the sequential data are usually parallel-spread in the frequency, time, and code domains of the carrier signals. Therefore, the realization of greater flatness for signal propagation properties within the authorized bands has become an important requirement for front-end devices. From the perspective of electromagnetic wave propagation, this means that the signal path (which is defined as the pathway between a wave source generating the modulated carriers and a receiver that demodulates them) must always be considered when determining the flatness. This point is considered to be an important practical and technical issue that must be resolved when constructing high-bit-rate communication systems.

One possible solution is to append to the transmitter and/or receiver a filter that compensates for frequency dependencies of the transmission properties of signal propagation paths. The conventional method for doing this involves the application of common digital filter technologies [1]. However, when much higher data transfer rates are needed, it is difficult for this solution to reduce the power consumption and its processing speed. Because the sampling rate of analog to digital converters should be considerably higher than the data rate, and because a fast calculation processor that does not affect the speed of data flow is indispensable. In order to avert the issues of realizing such a high-speed converter and processor with low power consumption, it is proposed in this paper that a passive filter should be used for the compensation, because the filter requires no power supply and processes signals by physical manner, therefore, the previously mentioned problems intrinsically never occur.

To compensate for the transmission properties of signal propagation paths, the passive filters required for this purpose must realize prescribed transmission properties in the time domain, namely simultaneous realization of the prescribed amplitude and phase responses in the frequency domain must be carried out. However, to the best of the authors' knowledge there is no general synthesis method for passive filters in the time domain. This paper, therefore, formulates an original synthesis method for such filters, based on traditional passive filter synthesis algorithms known as the coupling matrix synthesis method [5] and focusing on reconciling physical restrictions originate from linear response theory and basic properties of scattering matrices, where those restrictions must be satisfied in order to make the filters passive. The resulting method is sufficiently simple and flexible such that it can be applied to other areas such as general synthesis methods of microwave filters.

First, physical restrictions that must be satisfied by two-port

reciprocal passive circuits are presented in Section 2. Then, the basic idea for reconciling the restrictions is proposed in Section 3. Section 4 describes in detail the steps for the developed synthesis algorithms. Section 5 shows the concrete design of a filter compensating microwave propagation properties by following the developed algorithms after defining propagation path specifications. Future prospects for this method are discussed in Section 6.

2. RESTRICTIONS ON TRANSFER FUNCTIONS FOR TWO-PORT RECIPROCAL PASSIVE CIRCUITS

To explain the scope of the discussions developed later, some concepts are defined here. We assume that two distinct loci are connected to each other by some medium (wire or wireless) with a carrier of angular frequency ω (i.e., $\omega = 2\pi f$). For example, as shown in Fig. 1(a), in case of wireless communication systems, it is appropriate to define the signal propagation path (hereinafter "the path") as the entire signal path between a transmitter that generates modulated RF signals and a demodulator in a receiver. In this case, it is important to focus on frequency dependencies of the transmission properties of the path because they cause waveform distortions that degrade the data transfer rate. This is a consequence of overlapping of the tails of adjacent symbols. Therefore, all elements of the path — such as propagation paths, feed lines, antennas, and filters — should be considered.

In addition, it is also assumed that the linear and causal relationships between the transmitted and received signals always hold true. In other words, the path contains no other signal sources, frequency conversion devices, or feedforward control options. However, it may include amplifiers if its nonlinearity is negligible. With these assumptions, signal propagation properties can be described by the so-called classical control theory [2]. According to the theory, if input signals with waveform $I(t)$ emanating from one locus (i.e., the output port of the modulator in Fig. 1(a)) propagate through a path having transfer function $h(t)$, and are observed as output signals with $O(t)$ at the other locus (i.e., the input port of the demodulator in Fig. 1(b)), then $O(t)$ is given by the convolution of $h(t)$ and $I(t)$. Using Laplace transform, this can be described as $O(s) = h(s)I(s)$, where s is the complex angular frequency defined by $\mathrm{Im}s = \omega$.

It is observed that since $h(s)$ is usually dependent on s (i.e., $h(s) \neq$ constant), $O(s) \not\propto I(s)$. That is, waveform distortions are a natural occurrence, and degradation in the quality of the communication link is a direct result for wireless communication systems, although this argument also holds for the wired case. Therefore, to resolve

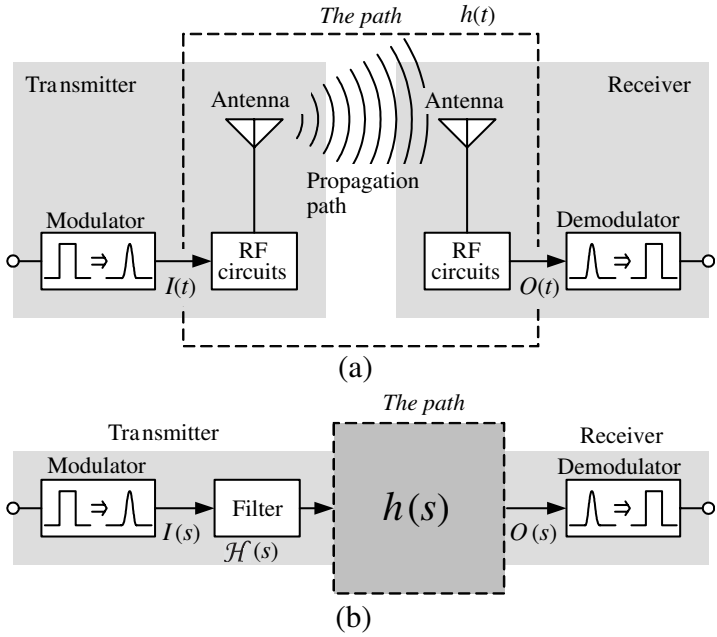

Figure 1. Compensation of frequency dependencies of the transmission properties of signal propagation path by inserting a particular passive filter. (a) Path in case of typical wireless communication systems. (b) Compensation by inserting a filter in the transmitter.

this problem without increasing energy consumption (mentioned in Section 1), it may be preferable to insert a specific "passive" filter that has the ability to eliminate the s dependency of $h(s)$ on the path, as shown in Fig. 1(b). As seen from the linearity of the system, one can insert the filter at any point along the path.

To construct a synthesis method for such a filter, we must first determine the properties of transfer functions for passive filters. From the control theory, the path and passive filters are classified as causal systems and the two-port transfer function $H(s)$ must obey the following four principal restrictions.

Restriction 1. $H(s)$ must be described as a certain rational function with finite polynomials for both its numerator and denominator. In addition, if the degree of the rational function $\deg H(s)$ is defined as the difference between the highest power of the

numerator n_n and that of the denominator n_d,

$$\deg H(s) \equiv n_n - n_d \leq 0 \tag{1}$$

must hold.

Restriction 2. The real and imaginary parts of $H(s)$ must be related to each other through the Hilbert transform.

Restriction 3. Every pole $\{\alpha_i\}$ of $H(s)$, namely solutions of an equation where the denominator polynomials are set to equal zero, must have a negative real part:

$$\mathrm{Re}\alpha_i < 0, \quad (i = 1, 2, \ldots, n_d). \tag{2}$$

Restriction 4. If it is postulated that scattering parameters (hereinafter S parameters) $\{S_{ij}(s)\}$ for a two-port reciprocal circuit are extracted from $H(s)$, the parameters must preserve the following two conditions, as shown in Fig. 2.

(i) **Cases 1 and 2:** In the cases of $S_{21}(s)$ and $S_{12}(s)$ (in the reciprocal case, $S_{21}(s) = S_{12}(s)$ holds), transmission zeros, which are defined as solutions of an equation where the numerator polynomials of $S_{21}(s)$ are set to equal zero, must be located on the imaginary axis of s or be mirror-symmetrically distributed in the two regions $\mathrm{Re}s < 0$ and $\mathrm{Re}s > 0$ with respect to the imaginary axes of s.

(ii) **Cases A and B:** Both sets of zeros for $S_{11}(s)$ and $S_{22}(s)$ must appear at the same positions on the imaginary axis of the s-plane or all the zeros for the parameters must be mirror-symmetrically distributed with respect to the imaginary axis and each pair of symmetrical points shared between the two parameters.

Here we explain the source of these restrictions. Restriction 1 describes a property of the so-called *proper transfer functions* [2], and ensures that future information never influences the present. Also, note that the reason for dealing with "proper" systems instead of "strictly proper" systems, where $\deg H(s) = 0$ is excluded, is that passive filters with $\deg H(s) = \deg S_{21}(s) = 0$ were actually constructed in [4, 6–8]. Restriction 2 is also a well-known consequence that is deduced from causality. The Hilbert transform can be described as the Laplace transform of $H(t) = \theta(t)H(t)$, where $\theta(t)$ is a unit step function defined as being equal to 1 if $t \geq 0$, and 0 otherwise. This restriction, therefore, requires that no output signal appears before the arrival of its corresponding input signals. Restriction 3 then states that $H(t) \to 0$ with a limit of $t \to \infty$, namely a specific weak energy conservation law. This basic understanding is derived from the pole analysis [9] for general passive filter synthesis methods. The last two restrictions are

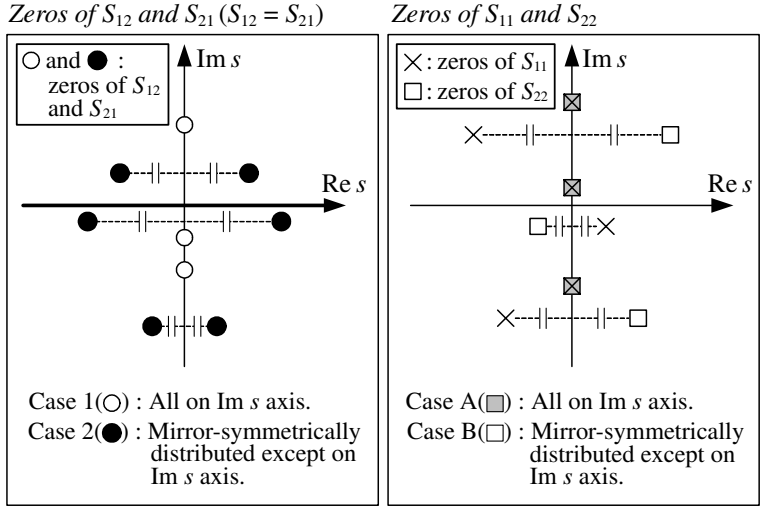

Figure 2. Restrictions imposed on the zeros of the S parameters for a two-port reciprocal passive circuit extracted from the transfer function.

indispensable for the construction of $H(s)$ as a real passive circuit. If the circuit is reciprocal, its S parameters must be a unitary matrix and the restrictions can be mathematically derived from that fact [3, 4, 6].

3. RECONCILING THE RESTRICTIONS

To construct passive filters with a specific transfer function and exclude any noncausal behavior, a synthesis method must be developed that fulfills all previously stated restrictions. This task is currently quite difficult because, from the viewpoint of the control theory, it can be deduced that the complete removal of the frequency dependency of proper systems equates to the construction of a time-reversing device. From the perspective of this paper (Fig. 1(b)), the dispersion of $h(s)$ is compensated for by inserting a passive filter with transfer function $\mathcal{H}(s)$ somewhere into the path. Because the complete transfer function of the path shown in Fig. 1(b) is $h(s)\mathcal{H}(s)$, setting $\mathcal{H}(s) = 1/h(s)$ therefore seems to be a plausible choice for realizing $h(s)\mathcal{H}(s) = 1$. However, such a $\mathcal{H}(s)$ cannot be constructed with passive circuits because of Restriction 1, since the path must be a strictly proper system and obey Restriction 1, $\deg h(s) < 0$. Then, $\deg \mathcal{H}(s) = -\deg h(s) > 0$ is deduced, showing that no passive circuit exists with such $\mathcal{H}(s)$.

In general, band limitations are imposed on most communication systems. Therefore, we can relax the condition that uniformity of the transfer function be realized only within authorized bands for the system. To this end, if we are content with obtaining uniformity of both amplitude and phase properties via passive linear phase bandpass filters [10, 11] in the finite frequency band, we can fulfill almost all of the stated restrictions. Namely, if we prepare a linear phase bandpass filter $L(s)$ and set

$$\mathcal{H}(s) \propto \frac{L(s)}{h(s)} \quad (\text{where } \deg L(s) < \deg h(s)), \tag{3}$$

it can be seen that linear phase responses and uniform attenuations in the authorized bands are realized. Also, since $\deg L(s) < \deg h(s)$, $\deg \mathcal{H}(s) < 0$ is deduced, the first restriction is assured.

The second and third restrictions can be simultaneously resolved by utilizing numerical approximation or fitting techniques for complex functions in order to synthesize $\mathcal{H}(s)$ as a rational function. For example, we previously obtained $h(s)$ by, for example, measurements of impulse response for the path, and assumed $L(s)$ to meet the specifications of the communication system to be established. In this case, if we directly synthesize $\mathcal{H}(s)$ obtained by (3) as a rational function satisfying the third restriction, then the second restriction is automatically fulfilled through the general properties of inverse Laplace transform. From the complex analysis, an inverse Laplace-transformed $\mathcal{H}(t)$ can become zero in $t < 0$ only if it has poles with negative real parts.

As shown in the next section, there are many candidates for the optimization synthesis method that are thought to be suitable for this purpose. However, it is difficult to impose conditions on the poles for the rational functions that are set as a fitting function in the approximation methods. Therefore, a type of nonlinear least square method is applied in this paper, since the loci of the poles directly become fitting parameters in this method, and the restrictions only limit regions in which they can exist.

The fourth restriction must be followed to construct $\mathcal{H}(s)$ as a passive filter. As can be easily seen, it is very difficult to reconcile the conditions for the zeros and poles of the S parameters and the third restriction. Because the two sets of points are strongly connected to each other with respect to the partial fraction expansion of rational functions, the simplest way to avoid this difficulty is to assume that $\mathcal{H}(s)$ has no zeros. Accordingly, no transmission zero of $\mathcal{H}(s)$ is assumed in this report.

Table 1. Synthesis algorithms.

Step	Content
1	Acquisition of transfer function $h(s)$ of the path for a prescribed communication system.
2	Determination of transfer function $\mathcal{H}(s) \propto L(s)/h(s)$ to compensate for $h(s)$, where $L(s)$ applies to a passive linear phase bandpass filter.
3	Transformation of $\mathcal{H}(i\omega)$ into its low-pass prototype $\mathcal{H}_{\mathrm{LP}}(i\Omega)$ and normalization of $\mathcal{H}_{\mathrm{LP}}(i\Omega)$ to yield $\mathcal{H}_{\mathrm{nor}}(i\Omega)$.
4	Optimization fitting of a rational function $\mathcal{H}_{\mathrm{pol}}(i\Omega)$ with $\mathcal{H}_{\mathrm{nor}}(i\Omega)$ by applying a nonlinear least square method.
5	Synthesis of two-port S parameters $\{S_{ij}(i\Omega)\}$ from $\mathcal{H}_{\mathrm{pol}}(i\Omega)$ using the coupling matrix synthesis method.
6	Extracting a filter circuit from $\{S_{ij}(i\Omega)\}$ according to specifications.

4. FILTER SYNTHESIS METHOD

In this section, the algorithmic flow of the proposed synthesis method for the previously mentioned filters is presented in detail, including mathematical manipulations, according to the outlines stated in the previous section. The algorithm is outlined in Table 1. Detailed discussions for each step are shown in the following subsections.

4.1. Step 1: Acquiring $h(s)$

We can consider several ways to perform this step, for example, the experimental observation of impulse responses or transmission properties for a wide frequency range and numerical simulations. Regardless of the method adopted, the raw data obtained usually contain the transmission properties of the path without dispersion. Therefore, it must be removed in order to subsequently use conventional filter synthesizing techniques. This can be easily accomplished by time shifting so that $h(t)$ begins to have nonzero values just at $t = 0$, as shown in Fig. 3. Assume that the observed raw transfer function is described as a product of the linear phase part and the remainder, namely $e^{-t_0 s}h(s)$, where t_0 is a specific positive real constant. On the basis of the linear response theory, $e^{-t_0 s}h(s)$ is identified as $h(t - t_0)$ in the time domain if $h(t)$ denotes the image of

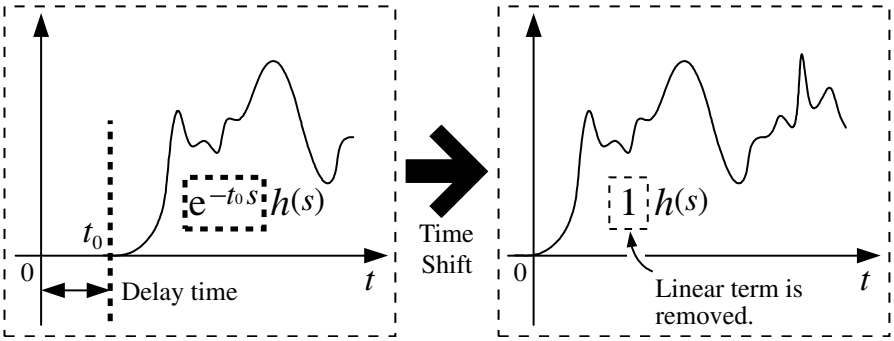

Figure 3. The linear term included in $h(s)$ can be removed by time shifting.

the inverse Laplace transform of $h(s)$. That is, $e^{-t_0 s}$ indicates a time delay of t_0. Therefore, such a linear term can be correctly removed only by redefining the origin of t in order to have a nonzero value at $t \geq 0$.

4.2. Step 2: Determining $\mathcal{H}(s)$

In this step, our aim is to determine $L(s)$ from the perspective of (3), focusing on the following points.

- Passbands for the linear phase filter must cover authorized bands for prescribed communication systems.
- $L(s)$ must have sufficient phase linearity to prevent another occurrence of waveform distortion, and should have no transmission zeros in order to satisfy Restriction 4 for S parameters.
- The degree of the filter must be determined so that the total phase change of the transfer function $\mathcal{H}_{\mathrm{LP}}(i\Omega)$ from $\Omega = -\infty$ to $\Omega = \infty$ satisfies

$$\angle\mathcal{H}_{\mathrm{LP}}(+i\infty) - \angle\mathcal{H}_{\mathrm{LP}}(-i\infty) < 0, \tag{4}$$

  where $\mathcal{H}_{\mathrm{LP}}(i\Omega)$ is a low-pass prototype transfer function for $\mathcal{H}(i\omega)$ defined by (3), and Ω is a low-pass (angular) frequency variable.

The first two points are trivial. However, the last point is explained below. It has already been agreed that $\mathcal{H}(s)$ must satisfy the restrictions stated above, particularly Restriction 3. We can, therefore, transform $\mathcal{H}(s)$ into its low-pass prototype $\mathcal{H}_{\mathrm{LP}}(S)$ (using a simple manipulation mentioned in the next subsection) and represent $\mathcal{H}_{\mathrm{LP}}(S)$ as a rational function of $\deg \mathcal{H}_{\mathrm{LP}}(S) = -N$, where N is a positive

integer, with no transmission zeros and poles with negative real parts (here $S = i\Omega$; strict definitions are given below):

$$\mathcal{H}_{\mathrm{LP}}(S) = c\prod_{i}^{N}\frac{1}{S-(a_i+ib_i)}, \quad (c\in\mathbb{C}, a_i<0)$$
$$= c\left(\prod_j r_j\right)\exp\left(i\sum_i^N \theta_i\right), \tag{5}$$

where $\tan\theta_i = \dfrac{\Omega - b_i}{a_i}$ and $r_j = \dfrac{1}{\sqrt{{a_j}^2+(\Omega-b_j)^2}}$. It can be easily recognized from (5) that

$$\angle\mathcal{H}_{\mathrm{LP}}(+i\infty) - \angle\mathcal{H}_{\mathrm{LP}}(-i\infty) = -N\pi < 0. \tag{6}$$

This is because, as shown in Fig. 4, since every θ_i asymptotically close to $\mp\pi/2$ at the limit of $\Omega\to\pm\infty$, the net values of $\angle\mathcal{H}_{\mathrm{LP}}(\pm i\infty)$ are equal to $\mp(\pi/2)\,N$. Therefore, the third point was derived. In addition, note that N represents the number of resonators that comprise the filter.

The negative definiteness of $\angle\mathcal{H}_{\mathrm{LP}}(i\Omega)$ within its passbands appears to be a sufficient but not necessary condition for practical use in filter synthesis. In general, low-pass prototypes are usually designed to have negative phase delay (which also means positive delay time) throughout their passbands. This is because it is difficult to construct actual filter circuits with positive phase delay. Such a delay can be realized using, for example, weak couplings between adjacent resonators in the main path and magnetic coupling structures [11].

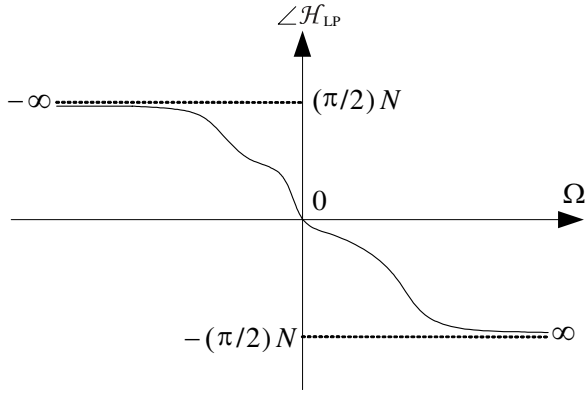

Figure 4. Asymptotic behavior of $\angle\mathcal{H}_{\mathrm{LP}}(i\Omega)$.

However, the former makes the filter unstable because it is easily influenced by its surroundings (especially the fluctuation in loads connected to filter ports), and the latter limits the magnification options of coupling constants for physically small filters such as microstrips. Following this line of reasoning, setting the strong condition

$$\angle \mathcal{H}_{\mathrm{LP}}(i\Omega) \lessapprox 0 \quad \text{(within passbands)} \tag{7}$$

appears to be a sensible choice, in addition to (6). As deduced from the previous discussion, (7) can be easily satisfied, and one can "renormalize" the noncausal properties of $1/h(s)$ if one uses a linear phase filter with a large enough number N of resonators. However, as the size of the filter increases, a tradeoff is required to determine an adequate N.

4.3. Step 3: Transforming $\mathcal{H}(i\omega)$ into a Low-pass Prototype Transfer Function $\mathcal{H}_{\mathrm{LP}}(i\Omega)$

A low-pass prototype is usually defined as a bandpass filter with cutoff $\Omega = \pm 1$. To maximize the use of conventional filter synthesis methods in the following steps, a low-pass transformation from $\mathcal{H}(i\omega)$ to $\mathcal{H}_{\mathrm{LP}}(i\Omega)$ is carried out. First, we obtain lower and higher cutoff frequencies from amplitude behaviors $\mathcal{H}(i\omega)$. In this step, the precise determination of passbands, such as the $-3\,\mathrm{dB}$ bandwidth, is not necessary, and all ambiguities are absorbed in the next step. Once a higher cutoff ω_H and a lower cutoff ω_L have been determined, one can obtain $\mathcal{H}_{\mathrm{LP}}(i\Omega)$ by performing the following frequency variable transformation,

$$\omega \to \frac{\Omega\Delta + \sqrt{(\Omega\Delta)^2 + 4}}{2}\tilde{\omega}_0, \tag{8}$$

where $\tilde{\omega}_0 = \sqrt{\omega_L \omega_H}$ and $\Delta = (\omega_H - \omega_L)/\tilde{\omega}_0$. Note that this is the inverse of the usual bandpass transformation [11].

If the low-pass prototype can be expressed as a lossless circuit with two ports having the same impedance, $S_{21}(i\Omega)$ must be proportional to $\mathcal{H}_{\mathrm{LP}}(i\Omega)$, and should have an amplitude of less than one ($|S_{21}(i\Omega)| \leqq 1$) in the entire band, and a phase of zero for the limit $\Omega \to 0$ ($\angle S_{21}(0) = 0$, which means that the DC gain of a passive filter must be a real number). Therefore, we must normalize the low-pass prototype $\mathcal{H}_{\mathrm{LP}}(i\Omega)$ by dividing its maximal value $\mathcal{H}^{\max}$ and its phase ϕ_0 at $\Omega = 0$ for $\mathcal{H}_{\mathrm{LP}}(i\Omega)$ as follows:

$$\mathcal{H}_{\mathrm{nor}}(i\Omega) = \frac{1}{\mathcal{H}^{\max} e^{i\phi_0}} \mathcal{H}_{\mathrm{LP}}(i\Omega). \tag{9}$$

4.4. Step 4: Fitting a Rational Function to $\mathcal{H}_{\mathrm{nor}}(i\Omega)$

After considerable preparations, a rational function that fulfilled the restrictions stated in Section 2 can be generated by applying numerical optimization techniques. In this paper, a type of nonlinear least square methods is applied. To begin, we prepare a rational function as a fitting function

$$\mathcal{H}_{\mathrm{pol}}(S) = c\prod_{i}^{N}\frac{1}{S-\alpha_i}. \tag{10}$$

Then, we define a specific positively defined function, for example,

$$\Delta(\boldsymbol{\alpha}, |c|) = \int d\Omega |\mathcal{H}_{\mathrm{nor}}(S) - \mathcal{H}_{\mathrm{pol}}(S)|^2, \tag{11}$$

as a cost function for the numerical approximation, where $\boldsymbol{\alpha} = \{\alpha_i\}$. To reduce the calculation cost, in practice, the integration in (11) may be replaced by a finite sum for the prescribed sampling points.

Note that (11) can also be defined as an integration in the time domain as opposed to the one in Ω. However, this frequently causes many local minima to originate from the oscillatory behavior of $\mathcal{H}_{\mathrm{nor}}(t)$ and $\mathcal{H}_{\mathrm{pol}}(t)$, and the stability of the optimization is greatly influenced by the choice of the overall sign of $\mathcal{H}_{\mathrm{pol}}(S)$. Optimization is realized by finding the global minimum of $\Delta\,(\boldsymbol{\alpha},\, |c|)$. In general, since the Hessian of the cost function does not always have positive eigenvalues (especially in our problem), optimization algorithms that are not significantly influenced by this (for example, the Levenberg-Marquardt method [14]) are appropriate.

When carrying out optimization in the manner described previously, a reduction in fitting parameters is required for the computing speed. If $\boldsymbol{\alpha}$ and c are selected and the number of real fitting parameters is $2N+2$, we can still reduce this number by one. Because the phase of $\mathcal{H}_{\mathrm{nor}}(S)$ at zero frequency was already set in a previous step, $\angle c$ can also be determined as

$$\angle c = \sum_{i}^{N}\angle\alpha_i - N\pi \tag{12}$$

by using the result of (6). With regards to α_i, they must be restricted beforehand to take on the values of (2) in the approximation algorithm.

We should recall that N, which is the degree of $\mathcal{H}_{\mathrm{pol}}(S)$ or the number of resonators composing the filter, has not yet been set. This is also determined using the result of (6). Namely, if one estimates the total number of phase changes from $\omega = -\infty$ to $\omega = \infty$, then N is

simply

$$N = -\frac{1}{\pi}\{\mathcal{H}_{\mathrm{nor}}(i\infty) - \mathcal{H}_{\mathrm{nor}}(-i\infty)\}. \tag{13}$$

Note that other approximation or interpolation techniques can be applied to this step. Examples are the Remez algorithm [12, 13] (also known as the osculatory interpolation method), rational interpolation methods (including Padé approximations) [15, 16], and infinite product expansion [17, 18]. However, the first two methods still have difficulties incorporating (2). The third method appears to be a plausible candidate because it has the potential to generate unique solutions, automatically taking the form of (10) and reconciling the previously noted restrictions via complex analysis.

4.5. Step 5: Synthesizing S Parameters $\{S_{ij}(S)\}$

In this step, we reproduce two-port S parameters for the filter from a previously obtained $\mathcal{H}_{\mathrm{pol}}(S)$. First, we assume that the filter is a lossless reciprocal passive circuit, and therefore, $S_{21}(S) \propto \mathcal{H}_{\mathrm{pol}}(S)$. With this assumption, we can approximate the representations for S parameters as

$$S_{11}(S) = \frac{F(S)}{E(S)}, \quad S_{21}(S) = \frac{1}{\varepsilon}\frac{P(S)}{E(S)}, \tag{14}$$

where $\varepsilon = 1/\sqrt{1-10^{-\mathrm{RL}/10}}$, as shown in [5]. Our next task is to determine the polynomials $E(S)$, $F(S)$, and $P(S)$ and the parameter RL according to the following procedures.

(i) RL is a free parameter that can be controlled by designers, and which defines the maximal return loss (in decibels) for S_{11} in the passband of the low-pass prototype. Therefore, one can specify RL, for example, as 20 dB.

(ii) Since $S_{21}(S) \propto \mathcal{H}_{\mathrm{pol}}(S)$, $P(S)$ and $E(S)$ can be easily identified from the result of (10) as follows:

$$P(S) = c, \quad E(S) = \prod_{i}^{N}(S - \alpha_i) \tag{15}$$

(iii) To determine $F(S)$, we utilize one of the unitary conditions for the S parameters describing lossless passive circuits, that is, $|S_{11}|^2 + |S_{21}|^2 = 1$. Inserting (14) into this formula, the following polynomial can be derived:

$$|F(S)|^2 = |E(S)|^2 - \frac{1}{\varepsilon^2}|P(S)|^2 \tag{16}$$

The specific polynomial of $|F(S)^2|$ can be given by inserting the preceding results (15) into the right-hand side of (16). $|F(S)|^2$ is a real coefficient polynomial of degree $2N$ in terms of the real variable Ω because of $S = i\Omega$. Hence, if $|F(S)|^2 = 0$, the equation has a total of N pairs of complex solutions for Ω that are related to each other by complex conjugation. We then denote the solutions as $\{\Omega_i^+, \Omega_i^-\}$ for $i = 1, 2, \ldots, N$. Here Ω_i^+ indicates one of the i-th pair of solutions with a positive imaginary part, namely $\mathrm{Im}\Omega_i^+ \geq 0$ and $\Omega_i^- = \overline{\Omega_i^+}$. As shown in Restriction 4. (ii), one is free to choose the solutions for constructing $F(S)$. Therefore, if we decide to select only those with negative real parts in terms of the Laplace variable S, we finally reconstruct $F(S)$ as follows:

$$F(S) = \prod_i^N \left(S - i\Omega_i^+\right) \tag{17}$$

Note that the choice of zeros for $S_{22}(S)$ is automatically set by Restriction 4.(ii) once the ones for the construction of $S_{11}(S)$ are chosen. We have finally completed the reconstruction of the S parameters from $\mathcal{H}_{\mathrm{pol}}(S)$.

4.6. Step 6: Extracting a Filter Circuit from *S* Parameters

The final step is performed simply by applying a general filter synthesizing method known as the "coupling matrix synthesis method" [4, 5]. The advantage of this method is its ability to determine all of the lumped parameters for a generic equivalent circuit composed of the multicoupled resonators from rational functions of $\{S_{ij}(S)\}$ in terms of the so-called "coupling matrix" M_{ij}. It is also able to provide a systematic reduction procedure that reduces the identified circuit to a specific filter configuration with prescribed circuit topologies. In the present problem, a filter without transmission zeros was assumed, as shown in (10). Therefore, the reduced circuit topology is expected to be a simple ladder without couplings among nonadjacent resonators. That is, nonzero elements of the matrix are only $M_{i,i}$ and $M_{i,i\pm1}$ for $i = 1, 2, \ldots, N$. The translation of the matrix M_{ij} into an actual filter is yet to be completed, but can be accomplished in line with ordinal filter synthesis, as shown in [11], for example.

5. PRACTICE OF SYNTHESIZING

In this section, the synthesis method proposed so far is demonstrated by designing a filter (hereafter "propagation properties compensation

filter" (PPCF)) for a specific signal propagation path. To begin defining path configurations, the filter will be synthesized by following the procedure proposed in Section 4.

5.1. Definition of a Signal Propagation Path and Determination of Its Transfer Function

We begin by defining a signal propagation path to be compensated for by a PPCF. As shown in Fig. 5, the path is a two-port radio propagation path that is designated by two antenna ports placed at a pair of identical oval-dipole antennas 6 m apart in free space, facing each other. Since the boresight direction of the antenna is normal to the substrate plane and the polarization direction of the emitted waves is parallel to the major axis of the elliptical pattern composing the antenna, Fig. 5 shows that both antennas are set up to maximize the received power. Since this propagation system is in free space and has no multipath signal, the nonuniformity of signal transmission properties is only due to the antennas' radiation dispersion and the distance attenuation.

Details of the antennas are given in Fig. 6. The configuration is the same as that originally shown in the manual for the Zeland IE3D ver.11.20 electromagnetic simulator [19], was applied in later calculations, and is suitable for an ultrawideband antenna. The antenna is assumed to be constructed of copper foil with a conductivity

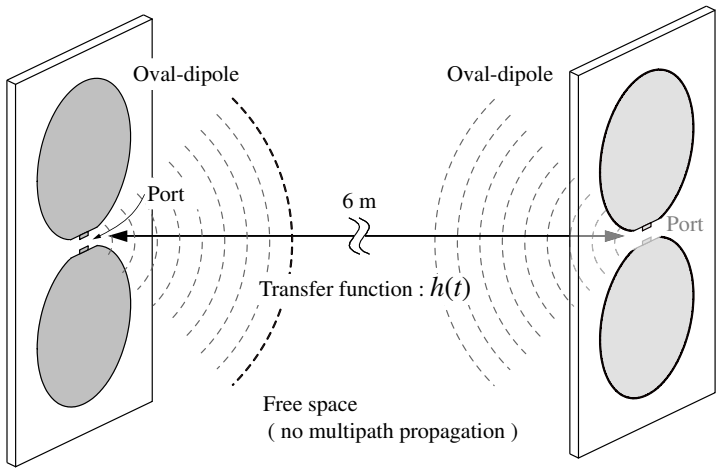

Figure 5. A signal propagation path composed of two identical oval-dipole antennas 6 m apart in free space and facing each other.

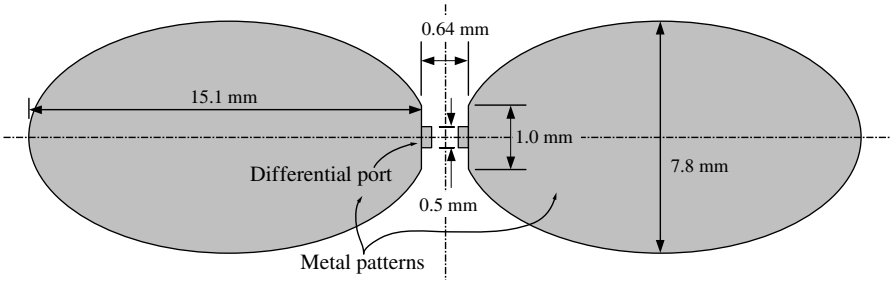

Figure 6. Detailed configuration of the oval-dipole antenna [19] composing the signal propagation path.

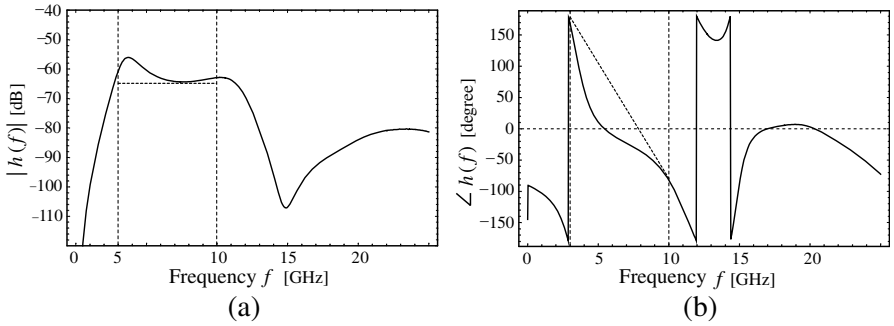

Figure 7. Frequency dependencies of $h(f)$. (a) Amplitude and (b) phase as calculated by the IE3D electromagnetic simulator. Note that a nonessential linear phase portion originally included in $h(f)$ has already been eliminated by the time-shifting technique, as stated in Section 4.1.

of 4.9×10^7 Sie/m and a thickness of 2 μm bonded on a dielectric substrate of permittivity 2.2, no loss tangent, and a thickness of 1.016 mm. Each antenna works as a single dipole with directivity as stated above. Therefore, its feeding port must be a differential input.

In this calculation, the transfer function of the path $h(f)$ (where f denotes frequency) is determined by applying numerical computations using the previously mentioned electromagnetic simulator for this system. The simulator can conveniently generate $h(f)$ directly from antenna properties obtained beforehand. Calculated results are shown in Fig. 7. A PPCF will be designed here to compensate for frequency dependencies of $h(f)$ between 3 and 10 GHz. Since the synthesis method stated in Section 4 is based strongly on conventional methods established for the narrow band theory, it might be not so rigorous to

deal with such a wideband RF circuit within the scope of this method. However, we will investigate this case as an example to illustrate the method. Our goal is to realize ideal propagation properties, namely uniform amplitudes and linear phase behaviors. Fig. 7 also indicates, using thicker dotted lines, the cases for which the frequency dependencies are perfectly compensated.

Note that an additional linear phase, which is caused by 6 m of nondispersive free space, and included in the original $h(f)$, has already been removed, and regulated results are shown in Fig. 7. This was carried out by transforming the original data into the time domain, time-shifting them so that the leading edge of $h(t)$ is correctly placed at the time origin, and then transforming them back into the frequency domain, as stated in Section 4.1.

5.2. Determination of the Target Transfer Function $\mathcal{H}(f)$ for a PPCF

In this step, we will determine a transfer function $\mathcal{H}(s)$ (where $s = 2\pi fi = i\omega$) to be obtained by an optimization-synthesized PPCF. This task corresponds roughly to the determination of an appropriate linear phase bandpass filter (LP BPF) that restricts the band for an intrinsically noncausal $1/h(s)$ in order to restore causality. The passband for the LP BPF is set as 3–10 GHz, as has already been stated. We must then set a filter order that is equal to the total number of resonators composing the LP BPF. Denoting the transfer function of the LP BPF as $L(s)$ and $\mathcal{H}(s) \propto L(s)/h(s)$, the order can be determined such that it satisfies a (strong) condition of $\angle\mathcal{H}(s) \lessapprox 0$ that holds within the passband for the PPCF, as stated in Section 4.2. However, we will attempt to slightly relax the condition and investigate its influence on the results. Here we will apply an eighth-order, maximally flat filter as the simplest choice. As long as such a BPF is adopted for the LP BPF, the preceding condition is slightly relaxed in a narrow band within the passband of the PPCF. This situation can be seen in Fig. 8. The slope of the phase curve for $\mathcal{H}(s)$ (Fig. 8(b)) becomes positive between 11 and 13 GHz, and the condition no longer holds. However, note that the condition will hold if the LP BPF is of sufficiently large order. Also, a real constant value is multiplied to normalize $\mathcal{H}(f)$, so that $|\mathcal{H}(f)|$ correctly has a maximal value of 1 in its passband.

It can also be seen that the amplitude of the resulting $\mathcal{H}(f)$ has significant values in the higher stopband of the LP BPF, namely between 10 and 15 GHz. This behavior results from small $|h(s)|$ values and insufficient attenuation of the LP BPF at its higher stopband.

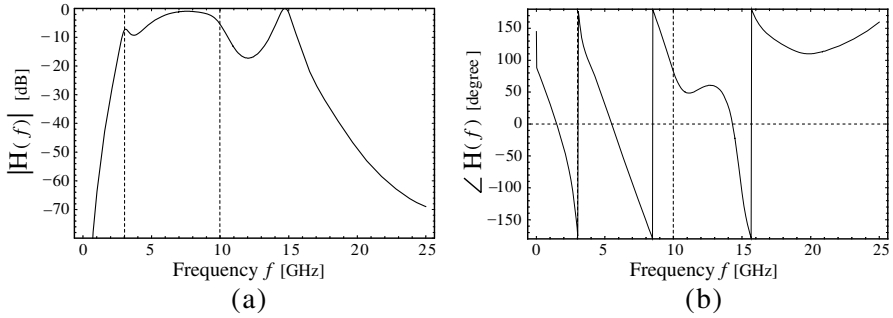

Figure 8. Frequency dependencies of the normalized transfer function $\mathcal{H}(f) \propto L(s)/h(s)$. (a) Amplitude and (b) phase of a PPCF. $L(s)$ represents the transfer function of an eighth-order, maximally flat filter with a passband of between 3 and 10 GHz.

5.3. Transformation of $\mathcal{H}(f)$ into Its Low-pass Prototype $\mathcal{H}_{\mathrm{LP}}(\Omega)$

To synthesize the PPCF with the previously determined $\mathcal{H}(f)$ as a rational polynomial, $\mathcal{H}(f)$ must first be transformed into its low-pass prototype $\mathcal{H}_{\mathrm{LP}}(f)$ because of the subsequent use of conventional filter synthesis methods that are based on low-pass circuits. Therefore, we must begin to determine a passband from Fig. 8. Note that the determination of the passband can be approximate because such roughness can be well absorbed in the next step. Lower and higher cutoff frequencies are approximated as $\omega_L/2\pi = 2.65\,\mathrm{GHz}$ and $\omega_H/2\pi = 15.2\,\mathrm{GHz}$, respectively. Then, using the low-pass transformation defined by (8), $\mathcal{H}_{\mathrm{LP}}(\Omega)$ can be obtained. The frequency dependencies are shown by the dotted curves in Fig. 9.

Figure 9 shows that the slope of the phase curve takes positive values near $\Omega = 0.85$, and that a sharp peak also exists in the amplitude curve in close proximity to the higher cutoff of $\Omega = 1$. In addition, as seen from the fact that the zero intercept of the phase of the $\mathcal{H}_{\mathrm{LP}}(\Omega)$ curve is not zero, the phase of $\mathcal{H}_{\mathrm{LP}}(\Omega)$ is not renormalized. In Section 4, it was stated that this renormalization should be performed to reduce the number of fitting parameters and to reduce the calculation cost. However, in this paper, we will set the phase as an overall constant in the next step because there are relatively few parameters.

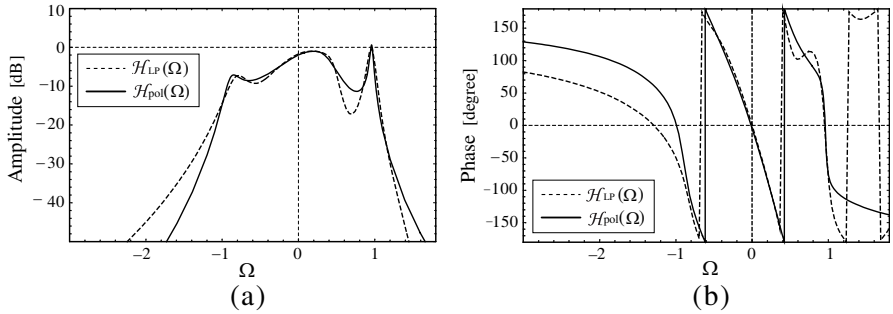

Figure 9. Frequency dependencies of a low-pass prototype $\mathcal{H}_{\rm LP}(\Omega)$ (dotted line) and optimization-synthesized $\mathcal{H}_{\rm pol}(S)$ (thick line) for the PPCF: (a) amplitude and (b) phase. Approximate cutoffs are set at $\Omega = \pm 1$.

5.4. Optimization Fitting of a Rational Polynomial $\mathcal{H}_{\rm pol}(S)$ to $\mathcal{H}_{\rm LP}(\Omega)$

We now fit a rational polynomial $\mathcal{H}_{\rm pol}(S)$, describing a corresponding causal system to the previously obtained $\mathcal{H}_{\rm LP}(\Omega)$ using numerical optimization techniques. In this calculation, the Levenberg-Marquardt method [14] is applied, with cost function $\Delta(\boldsymbol{\alpha}, c)$ defined by (10) and (11). Optimization is carried out by minimizing $\Delta(\boldsymbol{\alpha}, c)$, altering the loci of the transmission poles $\boldsymbol{\alpha} = \{\alpha_i\}$, and including the overall complex constant c as one of the fitting parameters. Note that one of the fitting parameters is chosen as c, and not as $|c|$, because to have zero in the previous step, $\angle\mathcal{H}_{\rm LP}(0)$ was not fixed.

First, we change the variable Ω to S by inserting $\Omega = -iS$ of the Laplace variable into $\mathcal{H}_{\rm LP}(\Omega)$ in preparation of the optimization. We must then determine a filter order N for the PPCF by using the formula

$$N = -\frac{1}{\pi}\{\mathcal{H}_{\rm LP}(i\infty) - \mathcal{H}_{\rm LP}(-i\infty)\}. \tag{18}$$

Figure 9(b) indicates that the total phase change of $\mathcal{H}_{\rm LP}(S)$ roughly equals -6π. Therefore, one can conclude that $N = 6$, and we can proceed to performing numerical optimization. After fitting $\mathcal{H}_{\rm pol}(S)$ to $\mathcal{H}_{\rm LP}(S)$, c and $\{\alpha_i\}$ are determined as shown in Fig. 10. Note that a sixth-order maximally flat filter and $c = 1$ are set as the initial conditions for optimization. The frequency dependencies of the resulting $\mathcal{H}_{\rm pol}(\Omega)$ are shown as thicker curves in Fig. 9.

As seen from Fig. 9, the optimization accuracy for both amplitude and phase is acceptable within the passband. However, upon closer

examination, it becomes worse in the neighborhood of a dimple close to the higher cutoff $\Omega = 1$ seen in Fig. 9(a). At these frequencies, it can be seen that the positive definiteness of the slope for the phase of $\mathcal{H}_{\mathrm{pol}}(S)$ no longer holds, and both curves for the amplitude and phase change sharply. Such behavior results mainly from a weakening of the negative definiteness condition of the slope for the phase of $\mathcal{H}(f)$. From this viewpoint, we should emphasize the conditions for higher-accuracy approximations. Therefore, adoption of considerably higher-order filters for the LP BPF is required.

Note also that the pole closest to the higher cutoff lies almost on the imaginary axis of S, and is isolated from the other poles, as shown in Fig. 10. This pole may be difficult to realize as a real filter circuit because it denotes a resonator with a very small energy loss and very weakly couples to other resonators. Therefore, this situation might be easily influenced by the surroundings, and the entire filter circuit may become unstable. This degradation is thought to occur because the order of the LP BPF is too low to suppress large values of $|1/h(f)|$. In addition to the utilization of higher-order LP BPFs, having $|1/h(f)|$ for the path not take on such large values is also an efficient way of preventing the occurrence of such isolated poles. Consequently, it can be deduced that antennas should have wideband frequency dependencies with respect to the amplitude of their directivity.

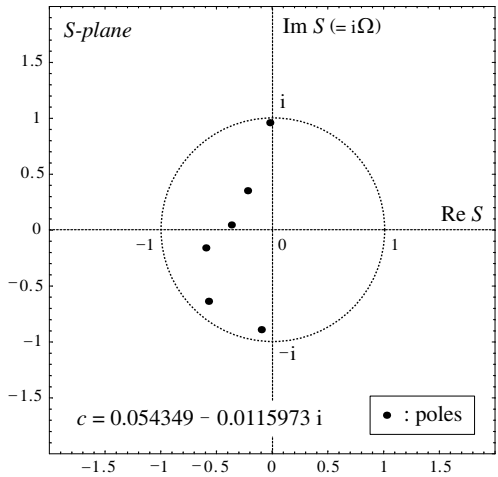

Figure 10. Transmission poles $\{\alpha_i\}$ determined by optimization and plotted on a complex S-plane with overall constant c for $\mathcal{H}_{\mathrm{pol}}(S)$.

5.5. Extraction of S Parameters from $\mathcal{H}_{\mathrm{pol}}(S)$

The next task is to extract S parameters $\{S_{ij}(S)\}$ as rational polynomials for a two-port lossless reciprocal passive circuit from the previously identified $\mathcal{H}_{\mathrm{pol}}(S)$. As stated in Section 4.5, this can be accomplished in a simple way using a conventional filter synthesis technique known as the matrix synthesis method [4, 5], and its ability to generate passive (or causal) circuits is guaranteed by the classical control theory [2], once $\mathcal{H}_{\mathrm{pol}}(S)$ is in the form of (10). Therefore, to accomplish this step, we must first determine the maximal return loss RL for S_{11} within the passband of the $\mathcal{H}_{\mathrm{pol}}(S)$ obtained above. In this calculation, it will be fixed at 20 dB. Then, following [4, 5], S_{11} and S_{21} can be extracted as follows:

$$
\begin{aligned}
S_{11}(S) &= \frac{F(S)}{E(S)}, \quad S_{21}(S) = \frac{1}{\varepsilon} \cdot \frac{P(S)}{E(S)}, \\
\varepsilon &= 1.00504, \\
P(S) &= 0.051831, \\
E(S) &= \{(0.0204514 - 0.960291i) + S\} \times \{(0.097599 + 0.890906i) + S\} \\
&\quad \times \{(0.21983 - 0.351433i) + S\} \times \{(0.367012 - 0.0465859i) + S\} \\
&\quad \times \{(0.571256 + 0.637579i) + S\} \times \{(0.595612 + 0.159844i) + S\}, \\
F(S) &= \{(0.00206941 - 0.958543i) + S\} \times \{(0.0918567 + 0.885963i) + S\} \\
&\quad \times \{(0.175858 - 0.28119i) + S\} \times \{(0.294239 - 0.101028i) + S\} \\
&\quad \times \{(0.571989 + 0.63446i) + S\} \times \{(0.604558 + 0.150357i) + S\},
\end{aligned}
$$

where the polynomial $F(S)$ is obtained by choosing solutions for the algebraic equation $|F(S)|^2 = 0$ in the second and third quadrants of the complex S-plane, as stated in Section 4.5. Also, frequency dependencies of $|S_{11}(\Omega)|$ and $|S_{21}(\Omega)|$ are shown in Fig. 11. As shown in Fig. 11, $|S_{11}|$ correctly has -20 dB as its minimum in the neighborhood of the higher cutoff, which corresponds to the isolated pole.

To confirm whether the frequency dependencies of the path are sufficiently canceled by the extracted S parameters, $h(f)$ (which is the transfer function for the path), $h(f)\mathcal{H}(f)$ (which are ideally compensated transmission responses which must equal that for the LP BPF $L(f)$), and $h(f)S_{21}(f)$ (which are the actual responses resulting from the insertion of the synthesized PPCF into the path), are overplotted in Fig. 12. As seen from Fig. 12, in the prescribed frequency range of 3–10 GHz, both frequency dependencies of amplitude and nonlinearity of phase for $h(s)$ are sufficiently improved, to the same extent as those for $L(f)$, as anticipated in Section 5.2. In addition, it is observed that weakening the negative definiteness condition for the phase of $\mathcal{H}_{\mathrm{LP}}(S)$ only affects the behaviors of the skirt at the higher

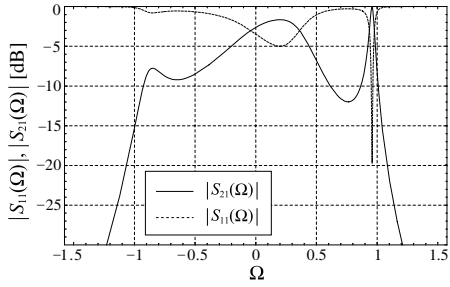

Figure 11. Frequency dependency of the amplitude for S parameters $S_{11}(\Omega)$ and $S_{21}(\Omega)$ synthesized from $\mathcal{H}_{\mathrm{pol}}(S)$.

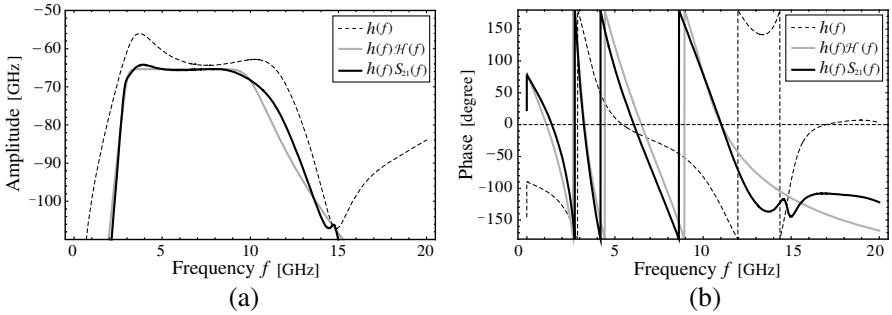

Figure 12. Frequency dependency of $h(f)$ (transfer function for the path), $h(f)\mathcal{H}(f)$ (ideally compensated transmission responses (equal to that for the LP BPF $L(f)$), and $h(f)S_{21}(f)$ (responses obtained by the insertion of the synthesized PPCF into the path): (a) amplitude and (b) phase.

cutoff band. Consequently, the PPCF is successfully synthesized and the effectiveness of the synthesis method is demonstrated.

5.6. Extraction of Filter Circuits from Synthesized *S* Parameters

The remaining tasks are to identify a coupling matrix M from the synthesized S parameters and to reduce M to its corresponding value for the prescribed circuit topology. Also, we need to determine two loads that terminate both ports of the circuit according to the methods shown in [4, 5].

In this case, since the PPCF is composed of six resonators, M must be a six-dimensional square matrix. We will show only the final

Table 2. Matrix elements of $(M)_{ij}$ $(i, j = 1, \ldots, 6)$.

No.	1	2	3	4	5	6
1	−0.16496	0.24595	−0.059488	−0.25744	0.27744	0
2	0.24595	0.072942	0.12396	0.46397	0.12027	−0.0083083
3	−0.059488	0.12396	−0.28897	−0.26422	0.60733	−0.21416
4	−0.25744	0.46397	−0.26422	0.61990	−0.099824	−0.74718
5	0.27744	0.12027	0.60733	−0.099824	−0.15428	−0.73189
6	0	−0.0083083	−0.21416	−0.74718	−0.73189	0.24539

Table 3. Matrix elements of $(M_{\mathrm{re}})_{ij}$ $(i, j = 1, \ldots, 6)$.

No.	1	2	3	4	5	6
1	−0.16496	0.45528	0	0	0	0
2	0.45528	−0.13147	0.64692	0	0	0
3	0	0.64692	0.018936	0.45818	0	0
4	0	0	0.45818	0.13885	0.51996	0
5	0	0	0	0.51996	0.22327	1.0677
6	0	0	0	0	1.0677	0.24539

outcome in Table 2 after performing the synthesis method. Table 2 clearly indicates that, since all matrix elements are nonzero, except for M_{16} and M_{61}, and since almost all resonators are correlated with each other, a circuit represented by such M is not practical. Therefore, we must reduce M to a simpler matrix according to [4, 5]. As stated in Section 4.6, $\mathcal{H}_{\mathrm{pol}}(S)$ having a transfer function of the same form as (10), namely with no transmission zeros, must be represented by an ordinal simple ladder circuit, that is, where each resonator is connected only to its two adjacent resonators. Therefore, the above M must be reduced to a matrix M_{re} that has nonzero diagonal elements and ones on each side of the diagonal. The reduced matrix M_{re} obtained by this method is shown in Table 3. Also, the loads R_1 and R_6, which terminate ports that are connected to the first and last resonators, respectively, are determined as follows:

$$R_1 = 0.065596, \quad R_6 = 1.8062.$$

One can determine the actual filter circuit even further from M_{re}. If one expects to obtain a circuit composed of only lumped elements, as shown in Fig. 13, their parameters can be directly derived from each

of the matrix elements $m_{ij} = (M_{\mathrm{re}})_{ij}$ through the following formulas:

$$\begin{aligned}
\tilde{R}_i &= \omega_0 R_i \Delta L && (i = 1, N), \\
L_{ii} &= \left(1 + \frac{1}{2} m_{ii} \Delta\right) L && (i = 1, \ldots, N), \\
C_{ii} &= \left(1 - \frac{1}{2} m_{ii} \Delta\right)^{-1} C && (i = 1, \ldots, N), \\
L_{ij} &= -m_{ij} \Delta L && (i, j = 1, \ldots, N, i \neq j),
\end{aligned}$$

where $\omega_0 = \sqrt{\omega_L \omega_H} = 1/\sqrt{LC}$ and $\Delta = (\omega_H - \omega_L)/\omega_0$. Note that all the lumped parameters can be calculated once a single parameter L is set. These formulas can be derived by calculating the first-order Taylor expansion of a loop equation [11] that represents the circuit shown in Fig. 13 with respect to an expansion variable ω, and imposing the condition that the approximated equation corresponds to the one expressed by the coupling matrix M_{re}. This derivation indicates that the equivalence of the generated lumped circuit to the corresponding loop equation only holds in a neighborhood of the expansion point ω_0. Consequently, the coupling matrix synthesis method is originally a narrowband theory. The one proposed here for PPCFs is based on the method, and is also justified within narrow bands.

If M_{re} is to be defined as a distributed circuit, the important parameters for this — namely, $k_{ij} (i, j = 1, \ldots, N,\ i \neq j)$, the coupling coefficients between resonators, $Q_i (i = 1, N)$, the external Q, and ω_i $(i = 1, \ldots, N)$, the resonant frequencies for each resonator — are

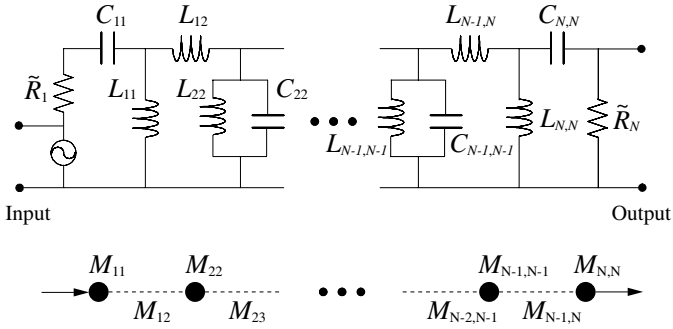

Figure 13. Definition of a circuit topology and notations of each element for synthesizing PPCF as a lumped filter.

given by the following formulas [11]:

$$k_{ij} = m_{ij}\Delta \qquad (i \neq j),$$

$$Q_i = \frac{1}{R_i \Delta} \qquad (i = 1, N),$$

$$\omega_i = \left(1 - \frac{1}{2} m_{ii}\Delta\right)\omega_0 \qquad (i, j = 1, 2, \ldots, N).$$

6. DISCUSSION

The proposed synthesis method generates PPCFs that compensate for frequency dependencies of a signal propagation path's transmission properties. This was fully illustrated by the practical design for an actual path. However, as stated above, short pulses spread out widely in the frequency domain, regardless of their waveform. Therefore, the authorized bandwidth for high-bit rate communication systems increases. The goal of the proposed synthesis method lies in the supply of filters that suppress signal path dispersion in the entire band, however, the method is based mainly on conventional filter synthesis techniques in the frequency domain. Therefore, more developments are needed to design such filters. Because the method applied in Step 6 is justified for the limit of narrow bandwidths (that is, lumped elements can be regarded as having no frequency dependency), if the treatment of lumped elements showing dispersion can be developed and subsequently incorporated into this method, the previously mentioned problem will be resolved. Recent wideband equivalent circuit modeling technique using circuit simulators and numerical fitting methods [20] might work well for this issue, even though a considerable amount of calculation must be required.

As seen from Fig. 12, the resulting phase behavior of the overall transmission after insertion of the PPCF has the same linearity as that of the LP BPF. Hence, phase behavior is dominated by the choice of transfer function for the LP BPF. If a communication system requires an even higher phase linearity, improvements in the properties of the LP BPFs, as shown in [11], should be considered.

7. CONCLUSIONS

A novel synthesis method for a class of passive filters that compensates for frequency dependencies of signal path transmission properties on the basis of the linear response theory and general properties of scattering matrices, was formulated. The method was successfully

demonstrated by carrying out the practical design of an assumed path composed of two oval-dipole antennas set 6 m apart in free space.

In the formulation of the method, restrictions for causal and energy-conserving passive systems were first determined and itemized. Then, to reconcile the restrictions, the regularization of the inverse of the transfer function of the signal path by multiplying it with a function of linear phase filters comprising a sufficient number of resonators, was proposed. An outline of the synthesis method for this idea was thoroughly discussed from the viewpoint of theoretical consistency. Synthesis algorithms were then proposed according to the considerations outlined, and the mathematical manipulations involved at every step were stated in detail. In the algorithms, the identification of the filter circuit from the determined functions can be performed in a straightforward manner by applying conventional numerical optimization techniques and the coupling matrix synthesis method.

Following the proposed method, after a transfer function for a two-port radio propagation path was calculated using an electromagnetic simulator, the filter was determined as a sixth-order simple ladder filter circuit through its reduced coupling matrix which is extracted from the transfer function. This was done in order to improve the uniformity of the path in the frequency range of 3–10 GHz. Finally, it was confirmed that the resulting filter compensated for the original transmission properties for the path to the same extent as the one for the eighth-order linear phase bandpass filter, assumed for regularizing the inverse of the transfer function for the path such that it is causal. Also, future developments in this technology were discussed.

REFERENCES

1. Li, G., "Recent advances in coherent optical communication," *Adv. Opt. Photonics*, Vol. 1, No. 2, 279–307, Feb. 2009.
2. Brogan, W. L., *Modern Control Theory*, 3rd Edition, Prentice Hall, New Jersey, 1990.
3. Collin, R. E., *Foundation for Microwave Engineering*, 2nd Edition, 254–255, Wiley, New York, 2001.
4. Cameron, R. J., "Advanced coupling matrix synthesis techniques for microwave filters," *IEEE Trans. on Microw. Theory and Tech.*, Vol. 51, No. 1, 1–10, Jan. 2003.
5. Cameron, R. J., "General coupling matrix synthesis methods for Chebyshev filtering functions," *IEEE Trans. on Microw. Theory and Tech.*, Vol. 47, No. 4, 433–442, Apr. 1999.

6. Amari, S., "Direct synthesis of folded symmetric resonator filters with source-load coupling," *IEEE Microw. Wireless Compon. Lett.*, Vol. 11, No. 6, 264–66, Jun. 2001.
7. Amari, S. and U. Rosenberg, "Direct synthesis of a new class of bandstop filters," *IEEE Trans. on Microw. Theory and Tech.*, Vol. 52, No. 2, 607–616, Feb. 2004.
8. Bairavasubramanian, R. and J. Papapolymerou, "Fully canonical pseudo-elliptic bandpass filters on multilayer liquid crystal polymer technology," *IEEE Microw. Wireless Compon. Lett.*, Vol. 17, No. 3, 190–192, Mar. 2007.
9. Helszajn, J., *Synthesis of Lumped Element, Distributed and Planer Filters*, McGraw-Hill, London, 1990.
10. Rhodes, J. D., "A low-pass prototype network for microwave linear phase filters," *IEEE Trans. on Microw. Theory and Tech.*, Vol. 18, No. 6, 290–301, Jun. 1970.
11. Hong, J. G. and M. J. Lancaster, *Microstrip Filters for RF/Microwave Applications*, Wiley, New York, 2001.
12. Henderson, R. K., L. Ping, and J. I. Sewell, "Extended Remez algorithms for filter amplitude and group delay approximation," *IEEE Proceedings G*, Vol. 138, No. 3, 289–300, Jun. 1991.
13. Jinno, T., Y. Saito, and M. Okuda, "A study on weighting scheme for rational Remez algorithm," *IEICE Trans. on Fundamentals*, Vol. E94.A, No. 4, 1144–1147, Apr. 2011.
14. Reich, J. G., *C Curve Fitting and Modeling for Scientists and Engineers*, McGraw-Hill, New York, 1991.
15. Press, W. H., S. A. Teukolsky, W. T. Vetterling, and B. P. Flannery, *Numerical Recipes in C*, 2nd Edition, Cambridge University Press, Cambridge, 1995.
16. Deschrijver, D. and T. Dhaene, "Fully parameterized macromodeling of S-parameter aata by interpolation of numerator & denominator," *IEEE Microw. Wireless Compon. Lett.*, Vol. 22, No. 6, 309–311, Jun. 2012.
17. Silverman, R. A., *Introductory Complex Analysis*, Dover, 1984.
18. Tseng, C. C. and S. L. Lee, "Design of variable fractional order differentiator using infinite product expansion," *Proc. 2011 20th European Conference on Circuit Theory and Design (ECCTD2011)*, 17–20, Aug. 2011.
19. "IE3D user's manual: Release 11," Zeland Software, Feb. 2005.
20. Wang, Y., J. Li, and L.-X. Ran, "An equivalent circuit modeling method for ultra-wideband antennas," *Progress In Electromagnetics Research*, Vol. 82, 433–445, 2008.